CDF/ANAL/TOP/CDFR/WXYZ

W mass resolution in $t\bar{t}$ events. A partial survey of the sources for uncertainty.

Wojciech Fedorko, Pekka K. Sinervo
University of Toronto

06 July 2003

1 Introduction

One of the most important physics goals of the second run of the CDF detector is the precision measurement of the mass of the top quark. In the run II we are operating in the environment where the systematic uncertainties will be the limiting ones. It is crucial to understand and minimize those uncertainties to make the best possible top mass measurement. The type of event, most convenient for top mass measurement is the lepton+4jets+missing Et. It may be possible to use the knowledge of the W boson mass to perform in-situ energy scale calibration in this kind of events. [Put in figure dMt Vs d MW?] This technique has been suggested as early as the design phase of the CDF II detector [**?**][TDR 2-8 1996]. To our knowledge there has been no attempt to explore this method. However several studies have been made which may be useful in developing the technique. In this note we present results which should be helpful in understanding if and how W mass information can be used to improve the top mass measurement. In this analysis we examine the effects that influence the W mass resolution in the ttbar events with one leptonic and one hadronic W decay. Among those effects are:

1. the effect of particles that fall outside of the jet system associated with the hadronically decaying W boson.
2. the effect of the central and 30 degree cracks.
3. the effect of other particles present in the event flowing into the jets associated with the W boson.

2 Methodology

2.1 Sample generation

We have generated 3M $t\bar{t}$ events using Herwig 6.400 [**?**] [**?**] based in the cdfsoft2 version 4.9.1. The collection of events was filtered. We require that one of the the W bosons

decays hadronically, while the other W decays leptionically. In addition we remove the events involving $W \rightarrow \tau + \nu_\tau$ decay. Full detector simulation was run on the remaining 850K events using the version 4.9.1hpt1 of cdf software. The primary vertex was forced to (0,0,0) in this sample. For this analysis only the Monte Carlo 'truth' and the calorimetry information was used, therefore to complete the 'Production' stage we have only run the CalorimetryModule and JetCluModule with the clustering radius set to 0.4.

2.2 Kinematic Cuts

We require that 4 jets with $E_T > 15GeV$ are present in the event. The JetClu module has no information about the type of the particle entering the calorimeter. If the leptonic W decay produces an electron we will have an additional jet object. Therefore we require that this 'jet' is uniquelly matched to the electron in the HEPG bank and we remove it from the jet collection. The E_T cut is applied after this operation. 487k events pass the cuts.

2.3 Jet to parton matching

We use the Montecarlo truth information to identify the qq' jets originating form the hadronically decaying W. The matching is performed in using similar procedure to the one used in [**?**]. Here we give an outline of the algorithm:

- For each jet in the jet collection we compute the $\eta - \phi$ distance R from the jet centroid to each of the major HEPG bank entities: the light quarks from the hadronically decaying W the b quarks and the lepton. If this distance is smaller than 0.4 we store the HEPG index of this parton. For light quarks as well as for the b quarks we use the HEPG entries corresponding to quarks after emission of the final state radiation.
- For both of the light quarks we store the indices of the jets whose centroid is within $R = 0.4$ from that quark.
- If a light quark is associated with only one jet and this jet has only one parton index stored -the index of the light quark at hand, we say that this parton is uniquelly matched to a jet.

For the purpose of our study we only consider the events where both light quarks are uniquelly matched to a jet. We have 424k such events.

2.4 Particle extrapolation

In each event we follow the HEPG bank starting with the light quarks. It is possible for the decay trees of the qq' pair to overlap. Some particles might be present in both the decay tree of a quark and its' 'partner' tree. There is no clear-cut way of assigning such 'common' particles to either one of the qq' jets. This situation arises due to the way the monte carlo generator simulates color flow in an event. Given this ambiguity we have decided to treat the qq' system as a whole and not to separate it artificially into jets at the generation/simulation level. Once the HEPG bank is followed to the last layer, the OBSP bank particles which originate from those HEPG particles are selected. All decays

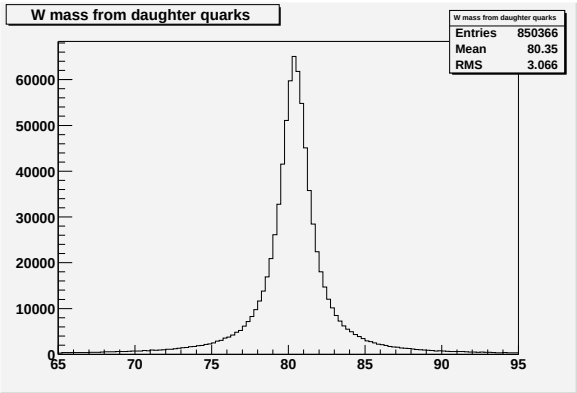

Figure 1: Generator level W mass obtained from the qq' system

in the OBSP bank are traced. For each particle in that last layer of the OBSP bank we compute the location of the calorimeter hit, taking into account the non uniform magnetic field and the position of its creation vertex. Once the position of calorimeter hit is known the tower indices are obtained. Using this method we are able to tell how many particles do not get clustered properly into jets and what is the energy that they carry away. We use the following procedure for determining those quantities:

- The collection of last layer of the OBSP particles originating from qq' is divided into three parts: collection whose origin is first quark; collection whose origin is the second quark; collection whose origin is ambiguous.
- In the case of the first two collections: For every particle in the collection we check if the tower hit by the particle is clustered into the jet uniquelly matched to the source parton. If the tower hit is clustered into the jet we say that the particle is found. Otherwise we classify the particle as missed.
- In the case of the last collection: For every particle in that collection we check if the tower hit by the particle is clustered in either of the qq' jets.

We use similar procedure to find what is the number of particles originating from the b quarks, the initial state radiation, the final state radiation emitted from the top quarks and the propagator radiation, and the energy that those particles carry into the jets associated with the qq' system. It should be noted that due to the color flow in the event those effects are not separable from one another on the generator level. That is large sets of particles common to several effects can exist. However the decay trees of ISR, FSR and b quarks are separated from the decay tree of the qq' system. This occurs since the qq' system is separated from the rest of the event by a colorless object -the W boson

3 Results and Discussion

Fig. 1 Fig. 2

Fig. 3 Fig. 4

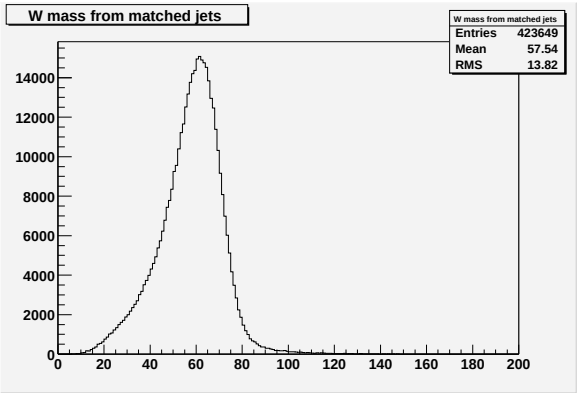

Figure 2: W mass obtained from the matched jets (uncorrected)

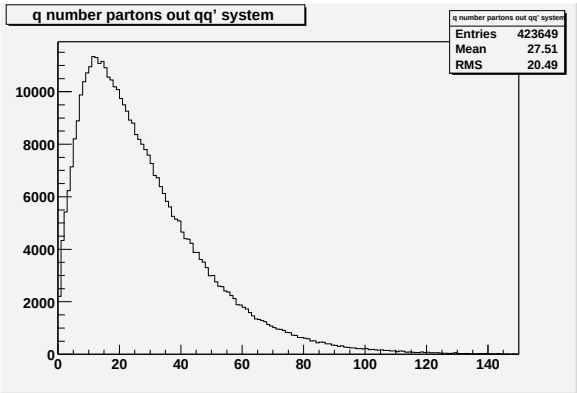

Figure 3: number of particles hitting towers not clustered in thw qq' jets

Fig. 5 Fig. 6

the categories F: fraction $> 0.6E : 0.4-0.6D : 0.3-0.4C : 0.2-0.3B : 0.1-0.2A : 0-0.1$

Fitting procedure: three iterations: first fit over the whole region than from $\mu - hwhm$ to $\mu + hwhm$ obtained from the previous iteration.

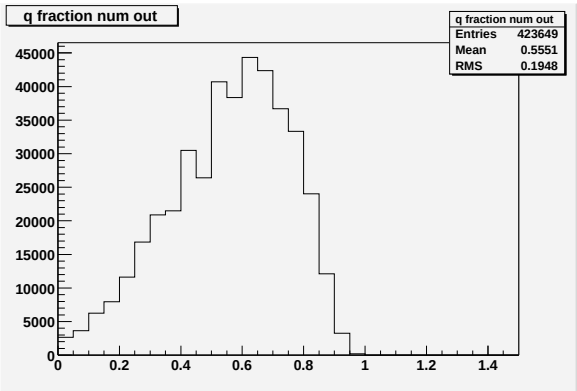

Figure 4: number of particles flowing out OVER total number of particles associated with the qq' system

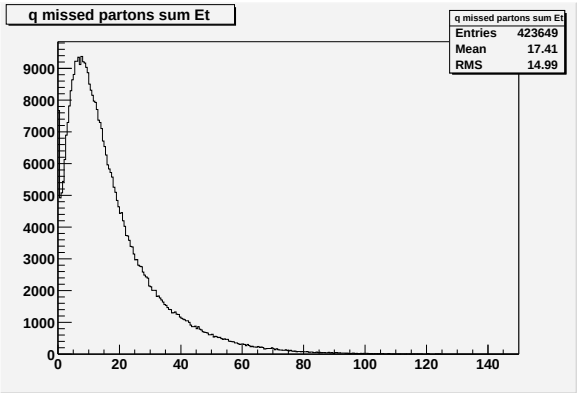

Figure 5: scalar sum of E_T carried away by the particles hitting towers not clustered into the qq' jets

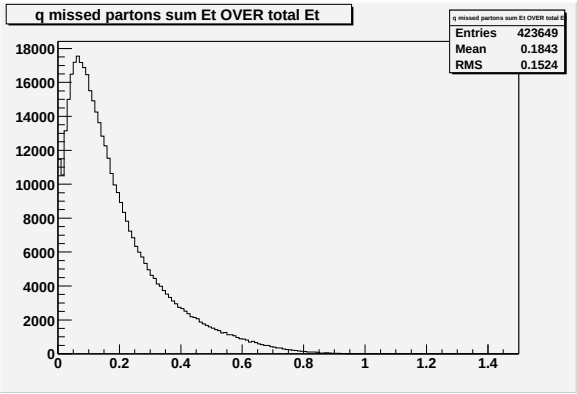

Figure 6: E_T sum of the misclustered particles OVER total scalar E_T sum of particles in the qq' system

Tail measure: $\frac{\int_0^{\mu - hwhm} w(m)dm}{\int_0^{200} w(m)dm} - \int_{-\infty}^{-\sigma\sqrt{ln(4)}} g(x)dx$ where $w(m)$ is the mass distro at hand and $g(x)$ is a perfect Gausian centered at 0 with stdev σ

Fig. 7

Fig. 8

Fig. 9

Fig. 10

Fig. 11

Fig. 12

Fig. 13

Fig. 14

Fig. 15

Fig. 16

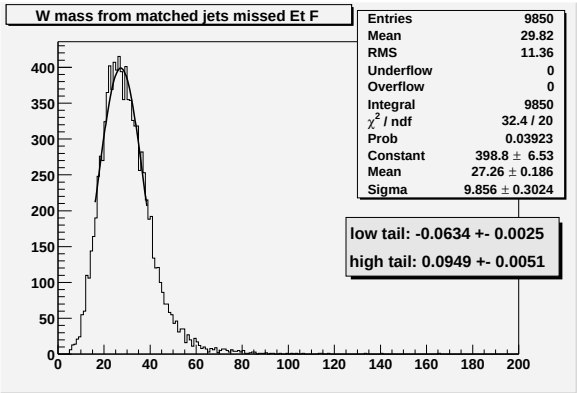

Figure 7: W mass resolution where the fraction of misclustered E_T is greater than 0.6

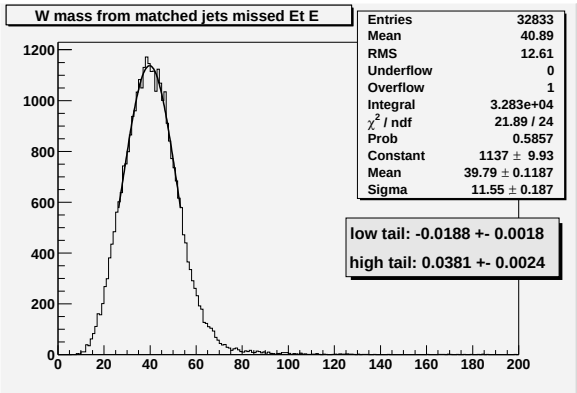

Figure 8: W mass resolution where the fraction of misclustered E_T is between 0.4 and 0.6

Fig. 17

Fig. 18

Fig. 19

Fig. 20

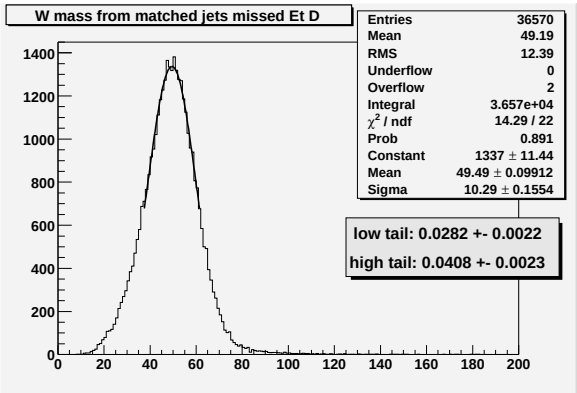

Figure 9: W mass resolution where the fraction of misclustered E_T is between 0.3 and 0.4

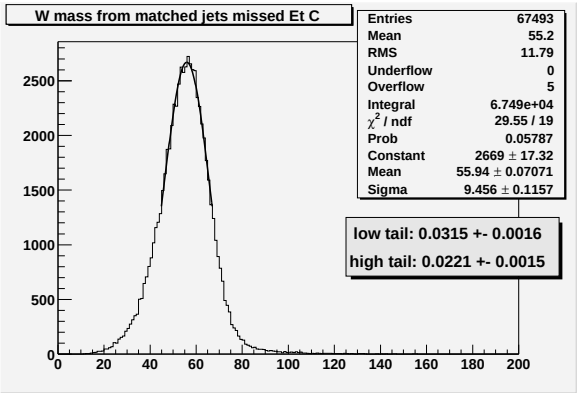

Figure 10: W mass resolution where the fraction of misclustered E_T is between 0.2 and 0.3

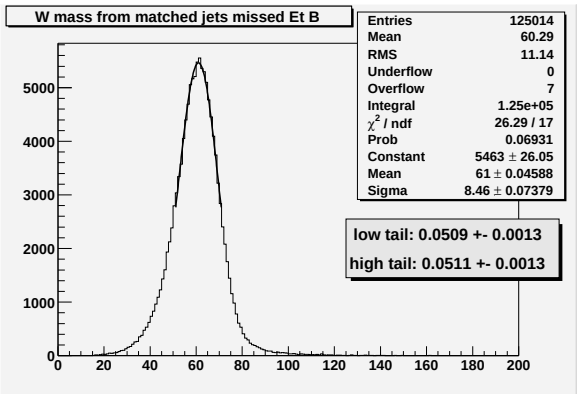

Figure 11: W mass resolution where the fraction of misclustered E_T is between 0.1 and 0.2

Fig. 21

Fig. 22

Fig. 23

Fig. 24

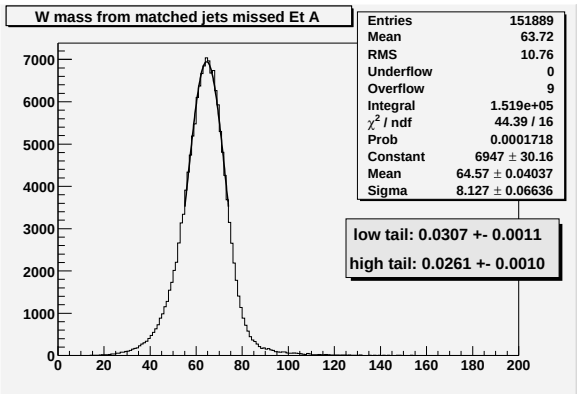

Figure 12: W mass resolution where the fraction of misclustered E_T is between 0 and 0.1

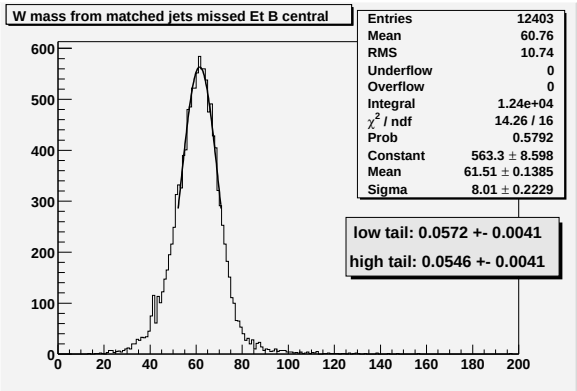

Figure 13: W mass resolution where the fraction of misclustered E_T is between 0.1 and 0.2 and both qq' jets are in the central region $0.3 < |\eta| < 0.7$

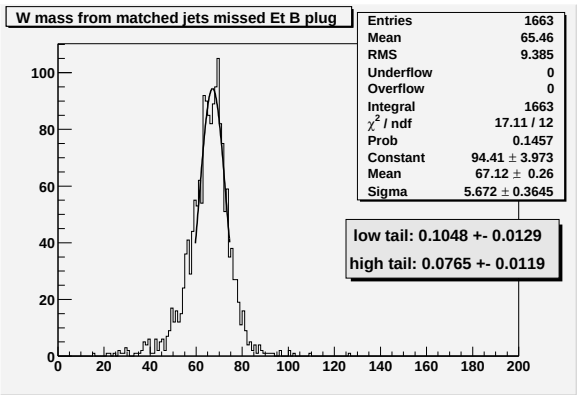

Figure 14: W mass resolution where the fraction of misclustered E_T is between 0.1 and 0.2 and both qq' jets are in the plug region $1.4 < |\eta| < 2.5$

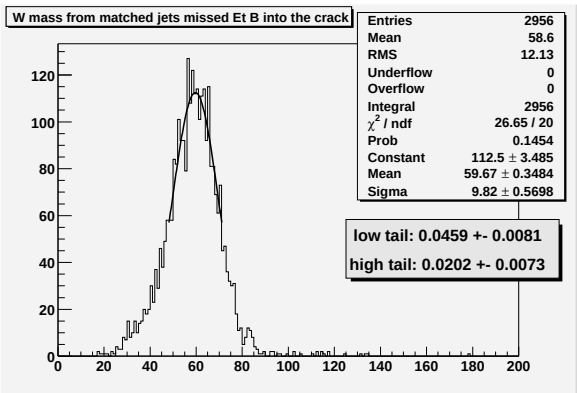

Figure 15: W mass resolution where the fraction of misclustered E_T is between 0.1 and 0.2 and both qq' jets are in the crack region $|\eta| < 0.1$ or $1.2 < |\eta| < 1.4$

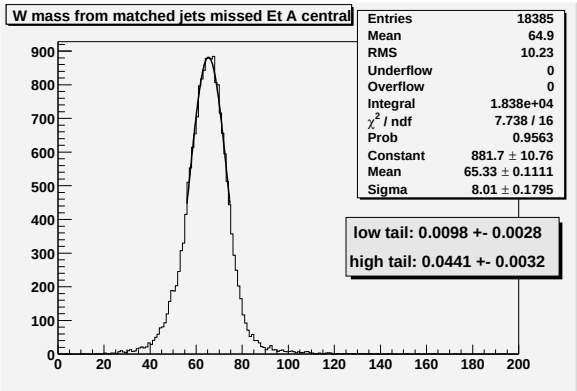

Figure 16: W mass resolution where the fraction of misclustered E_T is smaller than 0.1 and both qq' jets are in the central region $0.3 < |\eta| < 0.7$

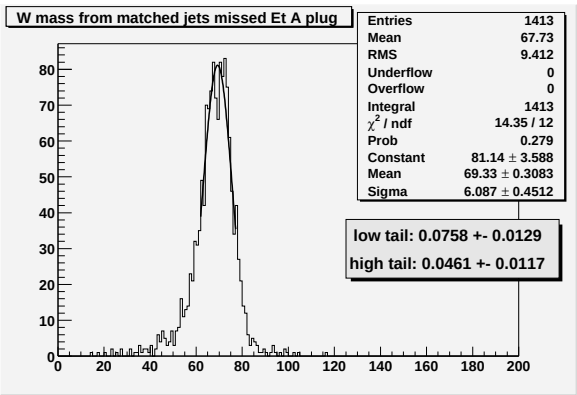

Figure 17: W mass resolution where the fraction of misclustered E_T is smaller than 0.1 and both qq' jets are in the plug region $1.4 < |\eta| < 2.5$

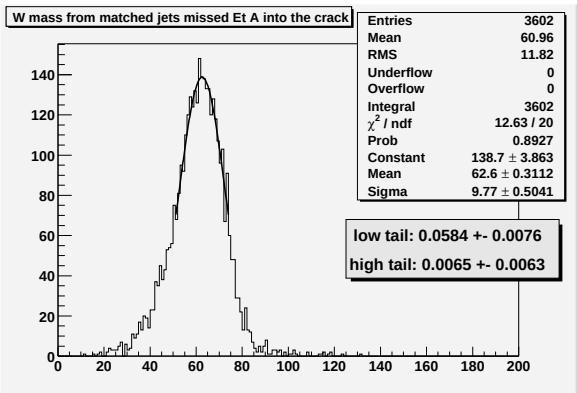

Figure 18: W mass resolution where the fraction of misclustered E_T is smaller than 0.1 and both qq' jets are in the crack region $|\eta| < 0.1$ or $1.2 < |\eta| < 1.4$

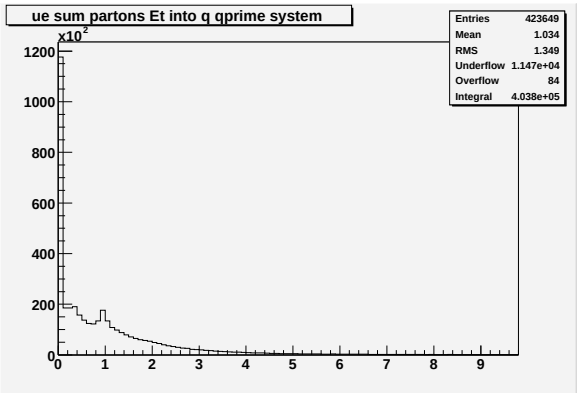

Figure 19: scalar E_T sum of the particles hitting towers clustered into the qq' system

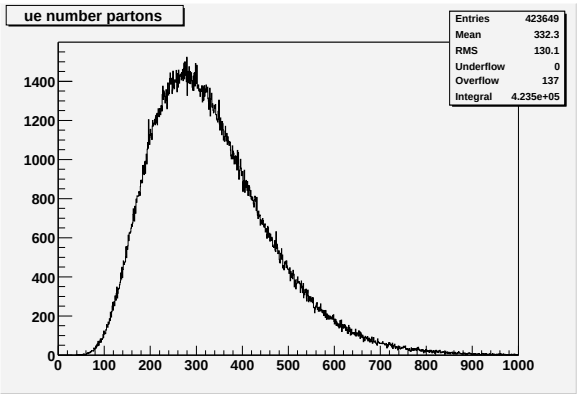

Figure 20: number of particles in the last layer of OBSP originating from ISR, top FSR, propagator radiation and b quarks

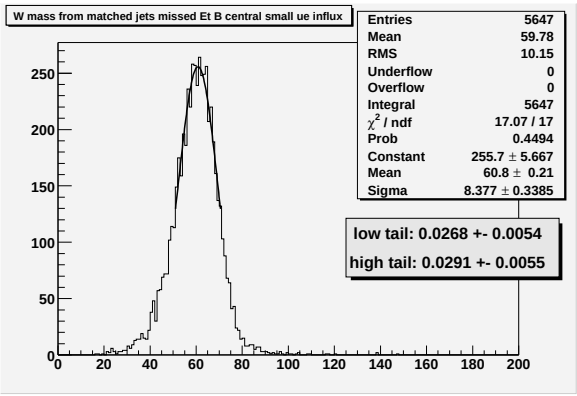

Figure 21: W mass resolution where the fraction of misclustered E_T is between 0.1 and 0.2 and both qq' jets are in the central region $0.3 < |\eta| < 0.7$ total E_T of particles flowing in from the underlying event + b $< 0.5GeV$

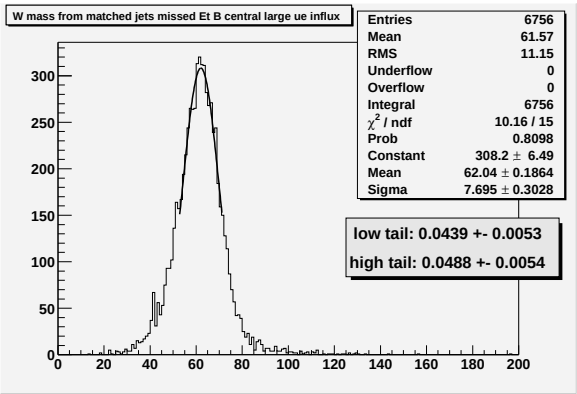

Figure 22: W mass resolution where the fraction of misclustered E_T is between 0.1 and 0.2 and both qq' jets are in the central region $0.3 < |\eta| < 0.7$ total E_T of particles flowing in from the underlying event + b $> 0.5GeV$

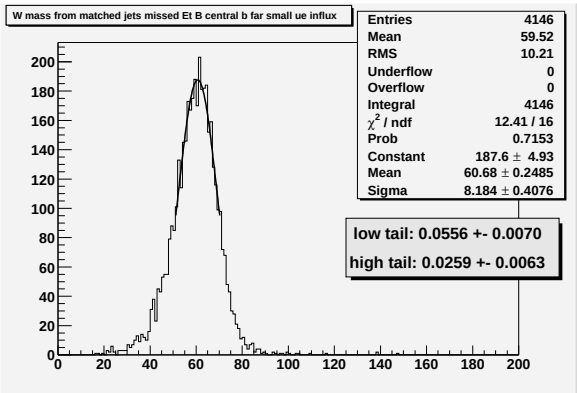

Figure 23: W mass resolution where the fraction of misclustered E_T is between 0.1 and 0.2 and both qq' jets are in the central region $0.3 < |\eta| < 0.7$ total E_T of particles flowing in from the underlying event + b $< 0.5GeV$ At the generator level b's separated from light quarks by radius at least 1.0

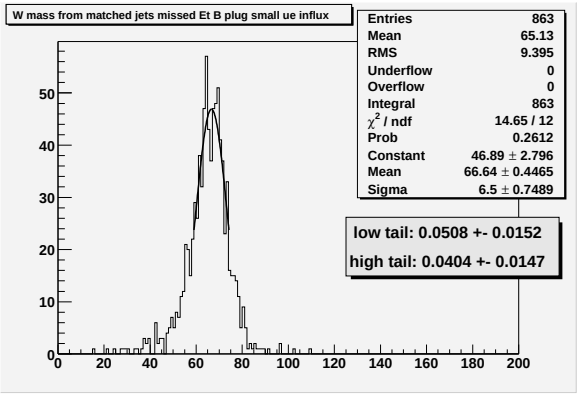

Figure 24: W mass resolution where the fraction of misclustered E_T is between 0.1 and 0.2 and both qq' jets are in the plug region $1.4 < |\eta| < 2.5$ total E_T of particles flowing in from the underlying event + b $< 0.5GeV$

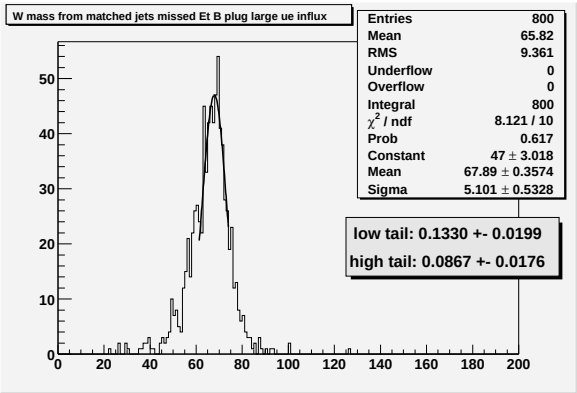

Figure 25: W mass resolution where the fraction of misclustered E_T is between 0.1 and 0.2 and both qq' jets are in the plug region $1.4 < |\eta| < 2.5$ total E_T of particles flowing in from the underlying event + b $> 0.5GeV$

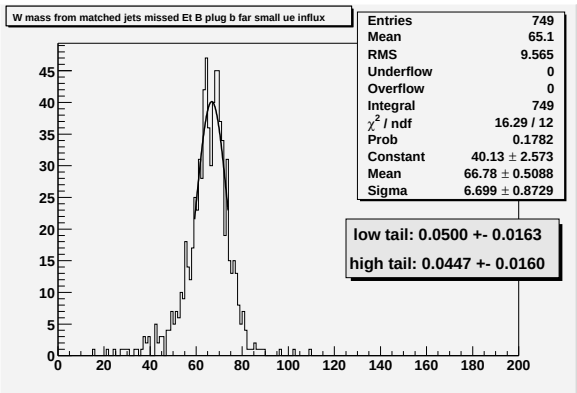

Figure 26: W mass resolution where the fraction of misclustered E_T is between 0.1 and 0.2 and both qq' jets are in the plug region $1.4 < |\eta| < 2.5$ total E_T of particles flowing in from the underlying event + b $< 0.5GeV$ At the generator level b's separated from light quarks by radius at least 1.0

Fig. 25

Fig. 26

Fig. 27 Fig. 28 Fig. 29 Fig. 30 Fig. 31 Fig. 32

[TDR 2-8 1996] G. Marchesini, B.R. Webber, G.Abbiendi, I.G.Knowles, M.H.Seymour and L.Stanco Computer Physics Communications 67 (1992) 465 G.Corcella, I.G.Knowles, G.Marchesini, S.Moretti, K.Odagiri, P.Richardson, M.H.Seymour and B.R.Webber, JHEP 0101 (2001) 010 ournote?

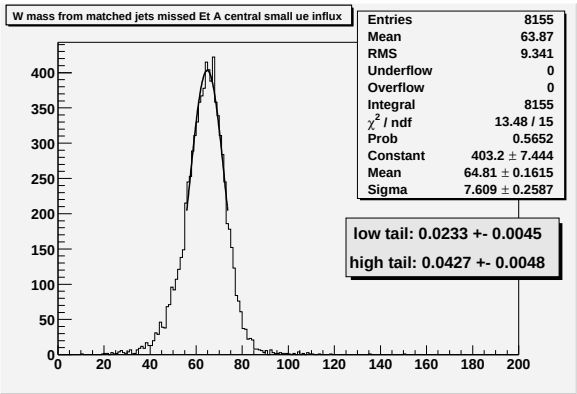

Figure 27: W mass resolution where the fraction of misclustered E_T is smaller than 0.1 and both qq' jets are in the central region $0.3 < |\eta| < 0.7$ total E_T of particles flowing in from the underlying event + b $< 0.5GeV$

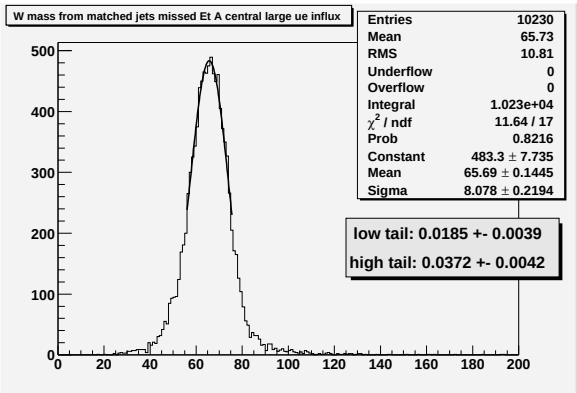

Figure 28: W mass resolution where the fraction of misclustered E_T is smaller than 0.1 and both qq' jets are in the central region $0.3 < |\eta| < 0.7$ total E_T of particles flowing in from the underlying event + b $> 0.5GeV$

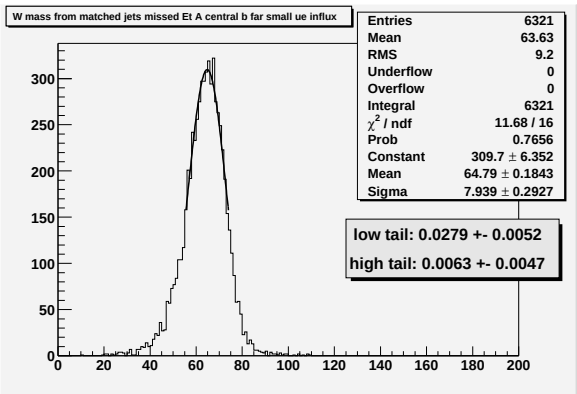

Figure 29: W mass resolution where the fraction of misclustered E_T is smaller than 0.1 and both qq' jets are in the central region $0.3 < |\eta| < 0.7$ total E_T of particles flowing in from the underlying event + b $< 0.5GeV$ At the generator level b's separated from light quarks by radius at least 1.0

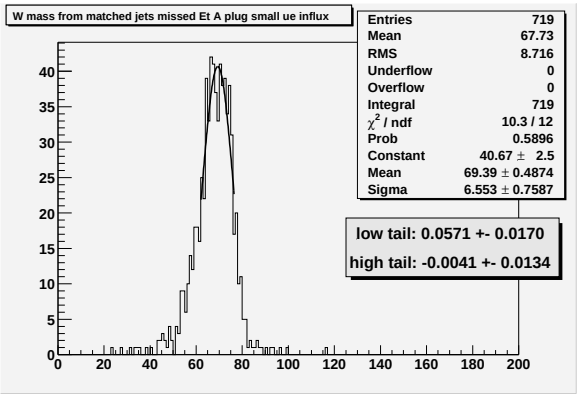

Figure 30: W mass resolution where the fraction of misclustered E_T is smaller than 0.1 and both qq' jets are in the plug region $1.4 < |\eta| < 2.5$ total E_T of particles flowing in from the underlying event + b $< 0.5GeV$

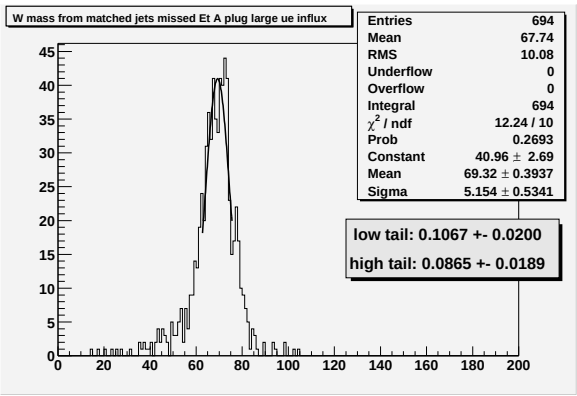

Figure 31: W mass resolution where the fraction of misclustered E_T is smaller than 0.1 and both qq' jets are in the plug region $1.4 < |\eta| < 2.5$ total E_T of particles flowing in from the underlying event + b $> 0.5GeV$

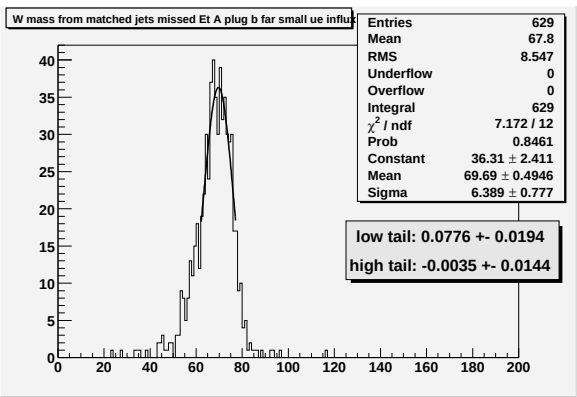

Figure 32: W mass resolution where the fraction of misclustered E_T is smaller than 0.1 and both qq' jets are in the plug region $1.4 < |\eta| < 2.5$ total E_T of particles flowing in from the underlying event + b $< 0.5GeV$ At the generator level b's separated from light quarks by radius at least 1.0